

To appear in the *Journal of Modern Optics*  
Vol. 00, No. 00, 00 Month 20XX, 1–15

## *Optical spectroscopic analysis for the discrimination of Extra-Virgin Olive-Oil*

N. McReynolds<sup>a</sup>, J. M. Auñón<sup>a</sup>, Z.Guengerich<sup>a</sup>, T.K. Smith<sup>b</sup> and K.Dholakia<sup>a\*</sup>

<sup>a</sup>*SUPA, School of Physics and Astronomy, University of St Andrews, St. Andrews, Fife, KY16 9SS, Scotland, UK* <sup>b</sup>*Biomolecular Sciences Building, University of St Andrews, North Haugh, St Andrews, Fife, KY16 9ST, Scotland, UK*

(v5.1 released December 2015)

We demonstrate the ability to discriminate between five brands of commercially available Extra Virgin Olive Oil (EVOO) using either the approach of Raman spectroscopy or fluorescence spectroscopy. Data was taken on both a 'bulk optics' free space system and on a compact hand-held device, each capable of taking Raman and fluorescence data. In the compact device we achieved a sensitivity and specificity of 98.4% and 99.6% for discrimination. Our approach illustrates that both Raman and fluorescence spectroscopy can be used for portable discrimination of EVOO's. This technique may enable detection of EVOO that has undergone counterfeiting or adulteration. The main challenge with this technique is that oxidation of EVOO causes a shift in the Raman signal over time. It would therefore be necessary to retrain the data base regularly. We demonstrate here preliminary data to an approach which may enable successful discrimination over time. We show that by discarding the first principal component, which contains information on the variations due to oxidation we can improve discrimination efficiency.

**Keywords:** Raman Spectroscopy, Fluorescence Spectroscopy, Extra Virgin Olive Oil, Oxidation

### 1. Introduction

Olive oil is an important part of the Mediterranean diet and is becoming increasingly more popular in North America due to its many known associated health benefits. It is produced from the fruit of the *Olea* tree using cold-press manufacturing methods that do not introduce chemicals or high temperatures. Extra virgin Olive oil (EVOO) is the highest quality of olive oil and must meet very specific standards; it is thus more expensive than other common edible oils such as vegetable oil. This often leads to adulteration of EVOO, where it is combined with cheaper, inferior oils and sold as genuine EVOO. This is particularly important in Asian countries where 'gutter oil' is produced and cause real food-safety concerns.

The International Olive Council (IOC) has established chemistry standards for the assessment of Olive Oil quality. The testing methods include analysing the Free Fatty Acid (FFA) content, the Peroxide Value, UV absorption at bands K232 and K268 and testing by a sensory panel.<sup>1</sup> These tests require skilled personnel and laboratory resources that are costly. Moving towards an inexpensive portable device for analysis would enable rapid and affordable analysis with minimal laboratory training.

Quality control is also a major challenge for the olive oil industry; ambient conditions such as temperature, light, and exposure to oxygen are key factors in the oxidation of olive oil, a major contributor to rancidity and chemical degradation. A study of the top five imported brands to California showed that 73% failed the IOC sensory standards.<sup>2</sup> Storage conditions, production and

---

\*Corresponding author. Email: [kd1@st-andrews.ac.uk](mailto:kd1@st-andrews.ac.uk)

transportation methods play an important role in the quality of olive oil, and is often the reason that many EVOO's are not of a good enough quality to be classified and sold as genuine Extra Virgin olive oil at the time of purchase. As oxidation is a self-catalytic process it is particularly important to monitor changes in the oxidation state of EVOO.

EVOO has thus become a major area of interest in the food technology industry, undergoing a wide variety of investigations in areas such as health benefits,<sup>3,4,5</sup> adulteration,<sup>6</sup> determining geographical origin,<sup>7</sup> and quality control.<sup>8,9,2,10</sup>

Raman Spectroscopy is a useful tool in chemical analysis as it can provide information on the chemical constituents of a sample in a non-destructive manner, without the need for sample preparation or the addition of chemicals. Raman Spectroscopy has already proved successful in Olive oil quality tests, providing information on the FFA content,<sup>11</sup> oxidation,<sup>9</sup> and adulteration of oils.<sup>6,12</sup>

However, a further important aspect would be the differentiation between different brands of olive oil based on a Raman or other photonics based approach, especially given the price differential that can arise between brands as a result of olive oil harvests and production for premium products in this market. Such discrimination can arise due to differences in chemical composition of olive oils, the main Raman peaks noted here correspond to the following vibrational modes:  $\nu(\text{C-C})$  ( $870\text{cm}^{-1}$  and  $1080\text{cm}^{-1}$ ), in-plane  $\delta(=\text{C-H})$  deformation in the unconjugated *cis* double bond ( $1266\text{cm}^{-1}$ ), in-phase methylene twisting motion ( $1301\text{cm}^{-1}$ ),  $\delta(\text{CH}_2)$  ( $1441\text{cm}^{-1}$ ),  $\nu(\text{C=C})$  *cis* ( $1646\text{cm}^{-1}$ ) and  $\nu(\text{C=O})$  ( $1747\text{cm}^{-1}$ ). These peaks can be used to identify oleic acid,<sup>19</sup> the main fatty acid in Olive oil, and are similar to those peaks observed in ref.<sup>6</sup>

Discrimination is also possible based on the variations of olive oil colour. It is worth commenting on the likely origin of such discrimination. The colour of olive oil may be attributed to various pigments which depend on the ripeness of the fruit, the soil or climate conditions and the extraction and processing procedures. For example ripe olives will have a higher content of carotenoids which produce a yellow oil. Green olives, however, have a high chlorophyll content producing a green oil. Chlorophyll and Pheophytin promote the formation of oxygen radicals in the presence of light and oxidation is associated with a yellowing of the oil. More vivid greens may be associated with the addition of twigs or leaves during grinding.<sup>13</sup>

It is instructive to explore whether either fluorescence alone or in combination with Raman can lead to appropriate discrimination for olive oils, which is the goal of this paper.

Standard Raman Spectroscopy suffers from a low signal to noise ratio (SNR), often accompanied by high autofluorescence background. Techniques such as Wavelength Modulated Raman Spectroscopy (WMRS)<sup>14,15</sup> have been developed to enhance the SNR. WMRS works on the principle of modulating the incident wavelength; any constant autofluorescence signal can thus be differentiated from a shifting Raman Signal and hence suppressed.<sup>16,17</sup> It is important to note here that when we take standard Raman data, there is no background subtraction, thus spectra contain both information from fluorescence background and Raman peaks; however when we take WMRS data any background fluorescence will be suppressed and only Raman peaks remain.

By acquiring and analysing fluorescence spectra, standard Raman spectra, and wavelength modulated Raman spectra we study the identification of various brands of EVOO. Our study demonstrates that fluorescence spectra alone can discriminate between 5 brands of EVOO. Solely focusing on Raman signatures using WMRS we are also able to discriminate between EVOOs. Standard Raman spectroscopy combines the Raman peaks with the background auto-fluorescence for discrimination and can also be used.

We have also observed subtle shifts in intensity of the Raman peaks on different days. It was found, by fatty-acid and methyl-esters (FAME) analysis, that this corresponds to oxidation of linoleic acid to form epoxides during storage. Linoleic acid is present in EVOO in small quantities but oxidises at rate an order of magnitude greater than that of oleic acid, due to the additional unsaturated bond. This however would reduce the efficiency of our discriminatory analysis in the absence of retraining, which limits the applicability of this technique. We have therefore investigated, preliminarily, a method of selecting of the most appropriate principal components for

analysis. This would enable us to reduce the significance of oxidation in discrimination of EVOO, and therefore to increase the robustness of this technique over a longer time frame.

## 2. Materials and Methods

Our analysis was performed on a large footprint apparatus as well as an ultra compact hand-held device. The free space apparatus was able to acquire both standard Raman data combined with background fluorescence, and modulated Raman data with background suppression. The hand-held device was only able to acquire standard Raman data. Solely fluorescence spectra were acquired using a miniature USB spectrometer and blue LED for illumination.

### 2.1. Instrumentation for Raman Spectroscopy

Two separate Raman spectroscopy systems were used, the first is a standard free space system similar to that described previously.<sup>18</sup> We used a tunable Ti:Sapphire laser (Spectra-Physics 3900s) operating at 785nm with maximum output power 1W. The laser was focused using a 50x 0.90NA oil immersion objective, delivering 145mW power to the sample plane. Raman scattered photons were collected through the same objective and detected by a monochromator (Shamrock SR-303i, Andor Technology) with 400 lines/mm, blazed at 850nm and a deep depletion, back illuminated and thermoelectrically cooled CCD camera (Newton, Andor Technology). Single spectra for standard Raman spectroscopy were acquired over 3s. The tunable laser allowed us to implement a WMRS approach to explore discrimination based solely on Raman signatures. A total modulation range of  $\Delta\lambda = 1.0nm$  was used. For WMRS five equidistant spectra were acquired of 3s each, totalling 15s per WMRS spectrum. Spectra were recorded over the wavenumber range of 800-1800 $cm^{-1}$ .

The second device used was a portable compact Raman Spectrometer, (model IDRaman mini, Ocean Optics), of dimensions 3.6" x 2.8" x 1.5". This system operates with a laser diode at 785nm. Spectra were acquired with an acquisition time of 500ms and laser power of 100mW. In this instance no wavelength modulation was achievable so the device recorded both the Raman and fluorescence signature at this wavelength. No base-lining of data was performed for this work and spectra were recorded over the wavenumber range 400-2300 $cm^{-1}$ .

### 2.2. Instrumentation for Fluorescence Spectroscopy

A blue LED of wavelength 473nm was focused into the centre of a standard cuvette holding 3ml of sample. A collection lens was positioned at 90° to the incident beam and light was then coupled into an optical fibre, leading to a mini USB spectrometer (model: USB2000+VIS-NIR, Ocean Optics) for detection. An acquisition time of 500ms was used.

### 2.3. Samples and sample preparation

Five brands of commercially available EVOO were purchased from the supermarket; Tesco's own brand, Napolina, Felippo Berio, Olea Maxima, and Peña de Martos. All bottles were opened at the same time and were stored at room temperature (298K), sealed, in a dark space.

Samples for the free space system were prepared using 2 quartz slides (SPi supplies, UK). The sample chamber well was constructed by placing a vinyl spacer of 80 $\mu m$  thickness on one of the quartz slides and loading 20 $\mu l$  of EVOO into the well. A thin quartz slide (0.15mm to 0.18mm thick) was used to seal the chamber. The slide was placed on the sample stage of the microscope with the thinner side closer to the objective. A total of 25 spectra were taken of each sample, moving the stage between each acquisition.

For the portable Raman device, a chamber above the laser diode held a small glass vial of 2ml volume, sealed with a plastic screw cap. To account for any variations between the glass vials a randomisation process was employed. Using 5 different vials per EVOO brand, 5 spectra were taken per vial; totalling 25 spectra per EVOO brand. Each vial was removed and reinserted to a new position between each measurement.

Samples were tested for effects of photo-bleaching by irradiating continuously for 10 minutes. There were no signs of signal degradation or burning.

#### 2.4. Data Processing

Data treatment was carried out using *Matlab 2014a*. All spectra were first normalised according to the area under the curve, to account for any power fluctuations in the laser. Principal component analysis (PCA) was conducted to achieve feature reduction of the data set. The ability to distinguish between EVOO brands was assessed using the method of leave-one-out cross-validation (LOOCV), where principal components (PCs) are defined using the entire data set except one spectrum. The left-out spectrum was then projected onto the principal component space and defined using the nearest-neighbour algorithm. Correct and incorrect predictions were summarised in a confusion matrix. The student's T test was also carried out pairwise at a significance level  $10^{-10}$  in order to highlight the main differences between two different EVOO brands.

WMRS spectra undergo a two step procedure; the five normalised spectra were first treated using PCA, where each wavelength is considered a different parameter. This produced a differential spectrum where zero crossing points represent Raman peaks. The differential spectra were then treated in the same manner as standard Raman spectra with PCA to reduce the data set to a few major variations.

The number of PCs used varies per system to optimise the amount of variability accounted for whilst minimising the number of PCs for faster processing. The free space system used the first 4 PCs: for standard Raman data this accounted for 99.7% variation and for WMRS data 94.1% of the total variance. For the portable device only 3 PCs were required, which accounted for 97.9% of the variance. For Fluorescence spectra the first 4 PCs were used corresponding to 77.3% of the total variance. Figure 1 illustrates the variance each of the first 5 PC's accounts for in all 4 setups.

#### 2.5. Fatty Acids of Methyl Esters (FAME) testing (to be updated by Terry Smith)

To understand the cause for intensity changes in Raman peaks on different days we investigated the lipids of each EVOO using FAME analysis, a technique using Gas Chromatography and Mass Spectroscopy (GC/MS). Lipids extracted from the five brands of EVOO were analysed 2 weeks apart.

Total lipids were extracted from the oil by the method of Bligh and Dyer; 100 $\mu$ l of EVOO was added to 100 $\mu$ l PBS in a glass tube. 750 $\mu$ l of 1:2 (v/v) CHCl<sub>3</sub>: MeOH was added and vortexed. The sample was agitated vigorously for a further 10-15 minutes. The sample was then made biphasic by the addition of 250 $\mu$ l of CHCl<sub>3</sub>. This was then vortexed and 250 $\mu$ l of H<sub>2</sub>O was added before being vortexed again. Finally the sample was centrifuged at 1000g at room temperature for 5 minutes. The lower organic phase was transferred to a new glass vial and dried under nitrogen until testing.

Both the organic and inorganic parts underwent Raman analysis to confirm changes in Raman peaks were due to changes in lipids.

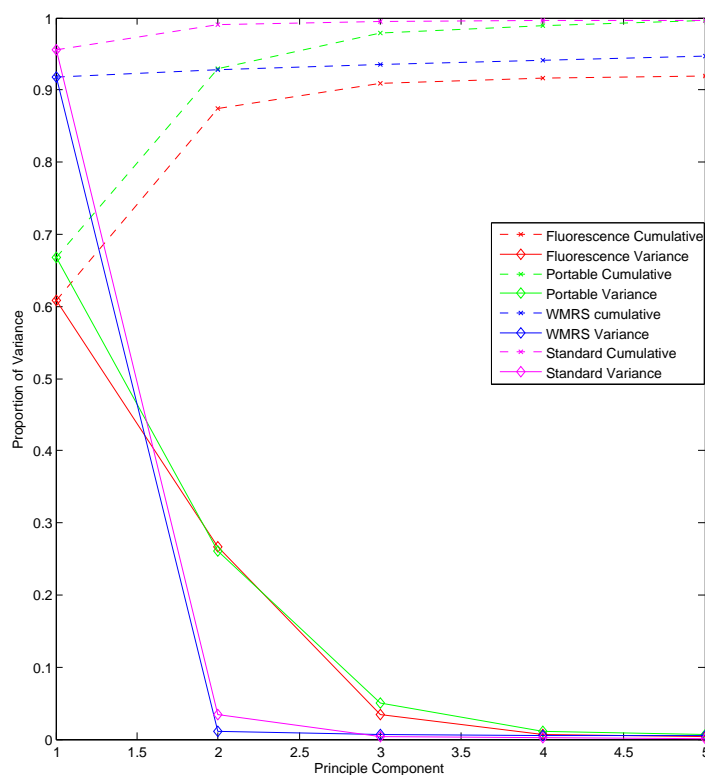


Figure 1. Scree plot to illustrate the proportional variance accounted for in the first 5 PCs for the following 4 systems; fluorescence only, the portable device, WMRS, and standard 'free space' Raman spectroscopy. Dashed lines represent the cumulative variance and solid lines show the individual contributions from each PC.

### 3. Results

#### 3.1. *Standard Raman Spectroscopy compared to Wavelength Modulated Raman Spectroscopy*

A comparison of standard Raman spectra from 5 brands of EVOO is shown in Figure 2. Grey bars are used to highlight regions of significant difference between spectra, as calculated by the students T-test at a significance level of  $10^{-10}$ . It can be seen that the main regions of significant difference between EVOO brands includes both background fluorescence levels and Raman Peaks. Plotting the loadings spectrally demonstrates that important contributions to the first PC, representing the most variability in the whole data set, come from Raman peaks at around  $1440\text{cm}^{-1}$ , between  $1260\text{-}1300\text{cm}^{-1}$  and at around  $1650\text{cm}^{-1}$ . The second largest PC has contributions from fluorescence between  $800\text{-}1100\text{cm}^{-1}$  and Raman peaks around  $1440\text{cm}^{-1}$  and  $1650\text{cm}^{-1}$ . PCA was

carried out on these spectra and well defined clusters representing the 5 brands of EVOO can be seen. A confusion matrix summing up the predictions from LOOCV is shown in Table 1, where diagonal components represent those correctly classified and off-diagonal components represent those incorrectly identified. Sensitivity and specificity values of 100% were achieved.

Figure 3 illustrates the differential WMRS spectra for the 5 EVOO brands and the principal component plots for the first three components. It can be observed that regions of significant difference correspond to the main Raman peaks and do not include any autofluorescence signals. This is consistent with the loadings, which are represented spectrally, where the flat baseline indicates that no fluorescence signal is included in the first two principal components. There are less regions of significant variation between 2 EVOO brands, consequently making it more difficult to successfully discriminate between them. This is also demonstrated in the nature of clustering in the PCA cluster plots, where clusters appear less well defined. The ability to discriminate using WMRS is summarised in Table 2, where diagonal values represent those correctly identified. The average pairwise sensitivity and specificity achieved for WMRS is 97.1% and 99.5% respectively.

Table 1. Confusion matrix for the differentiation of 5 EVOO brands using standard Raman Spectroscopy on the freespace system using the first 4PC's.

Prediction/Actual	1	2	3	4	5
1	25	0	0	0	0
2	0	25	0	0	0
3	0	0	25	0	0
4	0	0	0	25	0
5	0	0	0	0	25

Table 2. Confusion matrix for the differentiation of 5 EVOO brands using WMRS on the freespace system using the first 4PC's.

Prediction/Actual	1	2	3	4	5
1	25	0	0	0	0
2	2	23	0	0	0
3	0	0	24	0	1
4	0	0	3	22	0
5	0	0	2	0	23

### 3.2. Information from Fluorescence Spectroscopy

These results suggest that background autofluorescence from standard Raman spectra provides important information for identifying different brands of EVOO. We show that fluorescence signal alone is sufficient to discriminate between the 5 brands of EVOO. An inexpensive set-up was constructed to measure solely the fluorescence signal from the 5 brands of EVOO. The same methods for data processing were used. Figure 4 shows the normalised fluorescence signal acquired from the 5 brands of EVOO and the accompanying PCA cluster plots. Pairwise sensitivities and specificities of 100% were achieved in this study.

### 3.3. Portable Raman device for EVOO discrimination

The compact portable Raman device enabled discrimination between the five different brands of EVOO using standard Raman spectroscopy; combining information from fluorescence background and Raman peaks. The spectra are illustrated in Figure 5 alongside PCA cluster plots that show well defined regions for each EVOO. Spectral representation of the loadings illustrates that the most important contributions for the first PC, for differentiation between EVOOs, are the 7 Raman

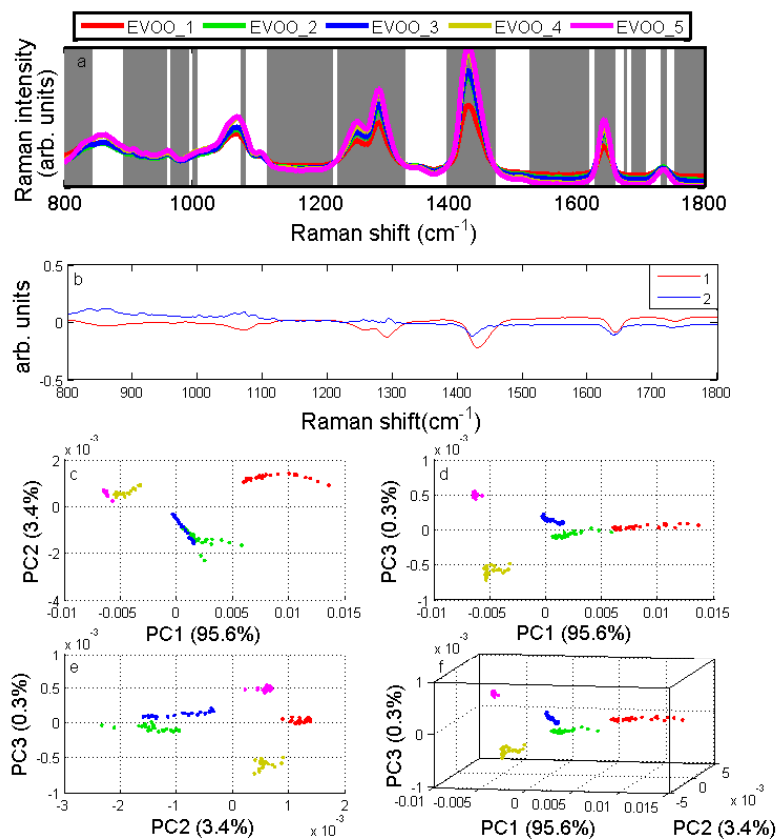


Figure 2. a) Spectra of 5 different brands of EVOO, solid lines represent the mean of each EVOO brand, shadowed regions represent the standard deviation. Grey vertical bars represent regions of significant difference between EVOO 1 and EVOO 2, as calculated by the student's T-test at a significance level of  $10^{-10}$ . b) Loadings for the first 2 PC's illustrate the variance contributions. c-f) Cluster plots representing the first three principal components. Each EVOO brand forms a well-defined cluster indicating they may successfully be differentiated.

peaks mentioned previously ( $870\text{cm}^{-1}$ ,  $1080\text{cm}^{-1}$ ,  $1266\text{cm}^{-1}$ ,  $1301\text{cm}^{-1}$ ,  $1441\text{cm}^{-1}$ ,  $1646\text{cm}^{-1}$ , and  $1747\text{cm}^{-1}$ ) and fluorescence in the region  $400\text{--}800\text{cm}^{-1}$ . The second largest variation mostly consists of fluorescence signal in the region  $900\text{--}1800\text{cm}^{-1}$ , with small contributions from Raman Peaks at  $1080\text{cm}^{-1}$ ,  $1301\text{cm}^{-1}$ ,  $1441\text{cm}^{-1}$ , and  $1646\text{cm}^{-1}$ . The third PC contains very little useful information. Table 3 quantifies the ability to identify EVOOs using the handheld Raman device, where diagonal values represent those correctly identified. The average sensitivity and specificity is 98.4% and 99.6% respectively, for pairwise comparison between EVOOs.

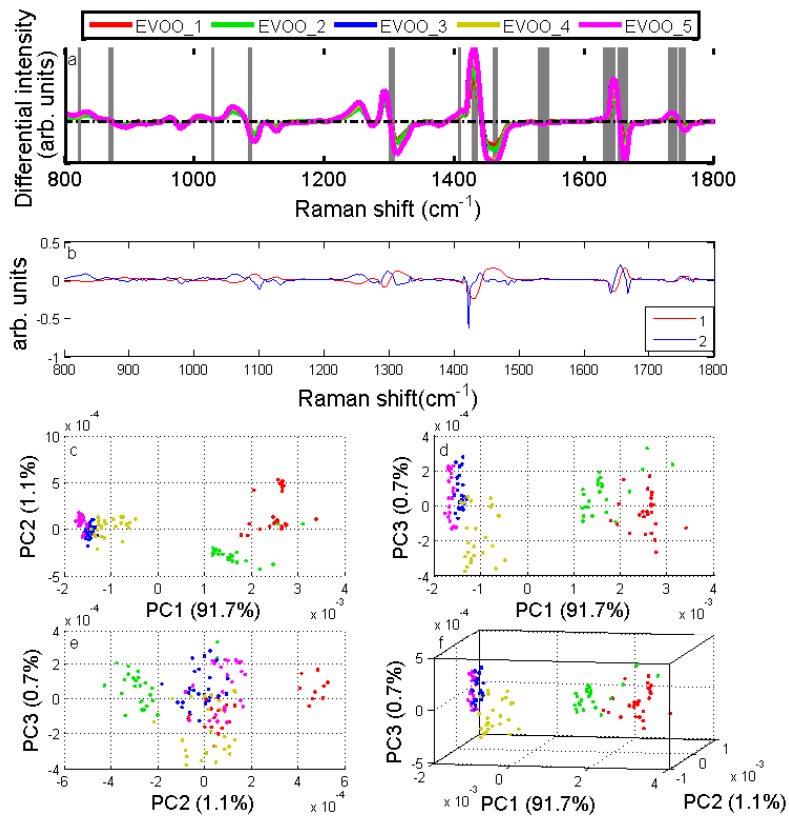


Figure 3. a) Differential WMR spectra of 5 different brands of EVOO, zero crossing points represent Raman Peaks. Solid lines represent the mean of each EVOO brand, with shadowed regions representing the standard deviation. Grey vertical bars represent regions of significant difference between EVOO 1 and EVOO 2, as calculated by the student's T-test at a significance level of  $10^{-10}$ . b) Loadings for the first two PC's illustrating variance contributions. c-f) Cluster plots representing the first three principal components. Clustering is less tightly formed than in standard Raman spectroscopy.

Table 3. Confusion matrix for the portable Raman device to differentiate between 5 brands of EVOO.

Prediction/Actual	1	2	3	4	5
1	24	1	0	0	0
2	2	23	0	0	0
3	0	0	25	0	0
4	0	2	0	23	0
5	0	0	0	0	25

### 3.4. Discrimination of EVOO on different days

It was observed that there is a change in the Raman signal with time, this can be seen in Figure 6 where the PC cluster is slightly shifted from its initial position. This is consistent across all



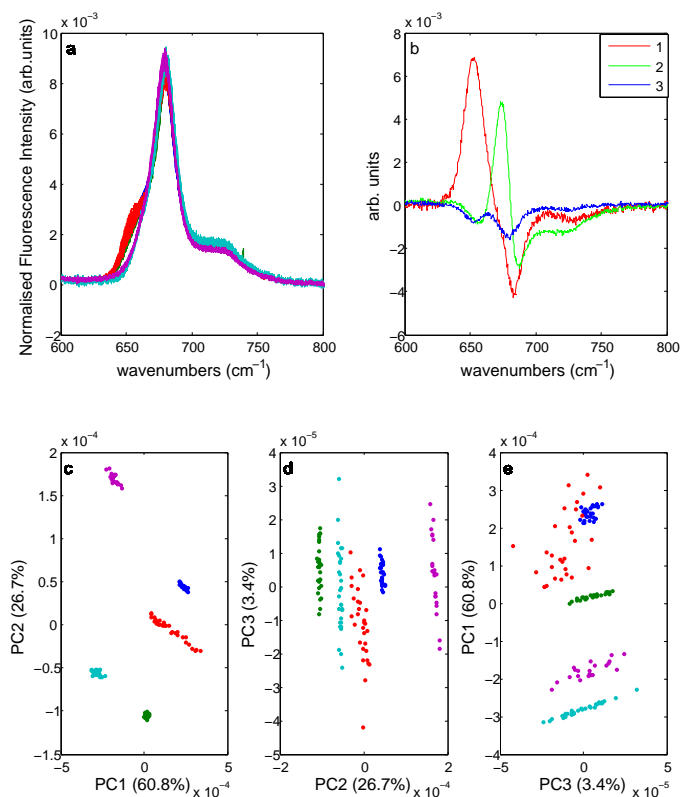


Figure 4. a) Normalised Fluorescence spectra from 5 brands of EVOO, b) Spectral loadings of the first 3 PC's, c-e) Cluster plots using the first 3 principal components. It can be seen that each brand forms a well-defined cluster illustrating the ability of fluorescence spectroscopy to differentiate between various brands of EVOO

brands of olive oil. Figure 6(a-b) demonstrates that we are sensitive to this shift over just one day, after opening the bottle, 6(c-d) demonstrates the shift on four separate days, over a total period of 10 days. Studies were conducted to confirm this does not correlate to a change in room temperature, pressure, or humidity. It is promising to note that the scatter plots shift along a continuous direction, and do not fluctuate back and forth. It may be therefore be possible to use this technique to measure the degree of oxidation for quality control. The data in figure 6 were obtained on the hand-held device although the effect was observed on all platforms.

To understand the cause of this shift, lipids were extracted from each brand of olive oil on week 3 and week 5, after opening the bottle, using the Bligh- Dyer method. The lipids underwent Raman spectroscopy, on the free-space system using standard Raman spectroscopy, and GC-MS. The PC plot showed a shift similar to that previously observed (see Figure 7b-c) suggesting the shift, even over one day, is indeed caused by chemical changes to the lipids. The corresponding changes in

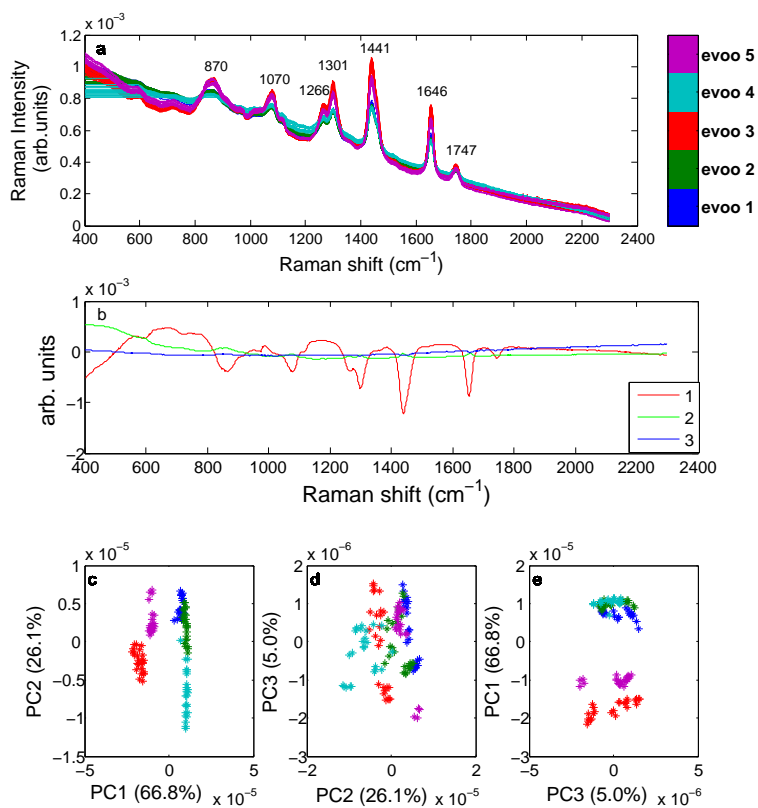


Figure 5. a) Spectra from 5 brands of EVOO taken on the portable compact Raman device. Raman peak positions are labelled. b) The first three loadings represented spectrally, illustrating variance contributions between EVOO brands c-e) PCA cluster plots using the first 3 principal components. Well defined clusters illustrate the ability of this device to differentiate between various brands of EVOO

Raman peak intensities are detailed in table 4 and can be clearly be seen in Figure 7a. Most notable is that in week three peaks corresponding to C=C double bonds are relatively more intense than week 5, and that in week 5 the Raman peak at  $1219\text{ cm}^{-1}$ , corresponding to Epoxy, is much larger than in week 3.

These results correspond well with the results from GC-MS. The peak at 39.55 mins (Figure 8), corresponding to linoleic acid, can be seen to decrease by 4.1 relative% in week 5 compared to week 3; and the peak at 43.85 mins, corresponding to epoxide, increases by 4.2 relative % in week 5 compared to week 3. All relative % changes can be seen in table 5. Although only EVOO 1 is presented here this is consistent across all 5 of the Olive oil brands.

In order to reduce the effect of the oxidation on our PC analysis and improve the robustness of our analysis over long periods of time we have investigated which of the first 10 PCs are optimal for discrimination. The changes due to oxidation are very strong and will be accounted for in the

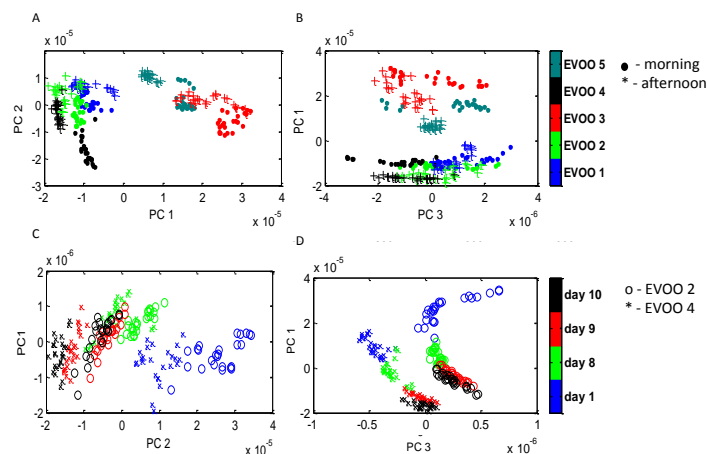


Figure 6. A-B) show the PCA scatter plots (PC1 V 2 and PC 1 V 3 respectively) for all 5 brands of EVOO with measurements taken on the morning and afternoon of the same day. C-D) demonstrates the drift in clusters for data taken on 4 separate days over a 10 day period. (only two brands of EVOO are displayed here to avoid confusion, where EVOO 2 is marked as 'o' and EVOO 4 is marked as '\*').

Table 4. Raman peak variations of lipids with time

Raman Shift ( $cm^{-1}$ )	description of change in week 5	vibrational bond
760	increased	$\nu$ C-C (aliphatic)
670	increased	$\nu$ C-C (aliphatic)
1219	increased	Epoxy
1740	increased	$\nu$ C=O
1085	decreased	$\nu$ C-C
1305	decreased	in-phase methylene twisting
1268	decreased	( $\delta$ =C-H) deformation in <i>cis</i> double bond
1443	decreased	$\delta$ cH
1654	decreased	C=C <i>cis</i> double bond

Table 5. Relative abundance of molecules on week 3 and week 5 for EVOO 1

Relative %	Wk3	Wk 5
C14:0	0.1	0.1
C16:0	17.1	17.3
C16:1	0.5	0.3
bran C18:0	5.8	5.7
C18:1(9)	47.4	47.9
C18:1(12)	2.6	2.5
C18:2	6.3	1.2
C20:0	0.4	0.3
C20:1(11)	14.5	14.7
C20:1(14)	0.1	0.1
C20:2	0.6	0.5
C18:1(epoxide)	0.1	4.3

first PC, however the remaining PCs each account for a very small percent of variation and so more are needed to enable successful discrimination. We have determined that using PCs 2 to 7 (accounting for 6.16% of all variation) is optimal with an average sensitivity of 99.7% and an average specificity of 99.7%. Using PCs 1-7 (accounting for 99.9% of all variation) gives sensitivity 99.7% and specificity 98.7%. This is summarised in Table 6 and 7 displaying confusion matrices for each method. This improvement shows that the drift caused by oxidation can be enough to

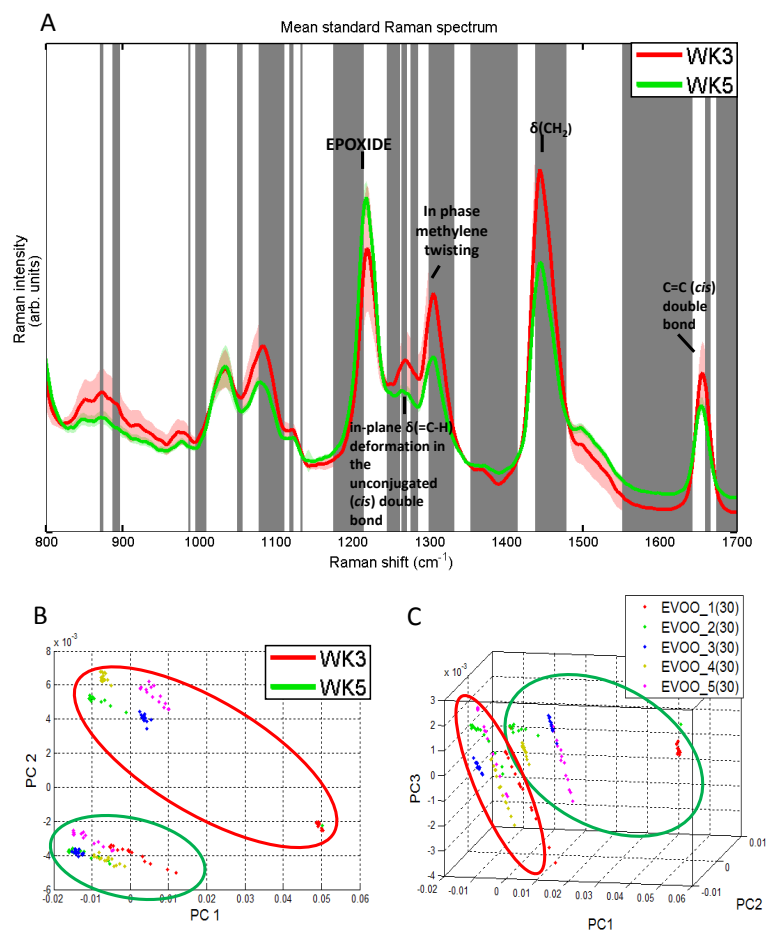


Figure 7. A) illustrates the average raman spectra for the lipids extracted from all 5 brands of olive oil on week 3 and week 5. The shadows indicate the standard deviation and grey vertical bars highlight regions of significant difference as calculated by the student's T-test at a significance level of  $10^{-15}$ . Week 3 has relatively more intense peaks corresponding to an extra unsaturated C=C bond, and week 5 shows an increase in the Raman peak at  $1219\text{ cm}^{-1}$ , corresponding to Epoxy. B-c Shows a shift in PC clusters from week 3 to week 5. Week 3 shows a larger range of variation as each brand shows differing degrees of oxidation. This is not so significant by week 5 when all brands have underwent oxidation.

cause some confusion between data taken at different times. This is only preliminary data as a much more interesting study would involve a larger data set over a much longer period of time and with some samples more strongly oxidised through intentional exposure to open air, higher temperatures, or light.

Table 6. Confusion matrix for data taken over 2 weeks using PCS 1-7

Prediction/Actual	1	2	3	4	5
1	29	1	0	0	0
2	1	26	1	2	0
3	0	0	30	0	0
4	0	0	0	30	0
5	0	0	0	0	30

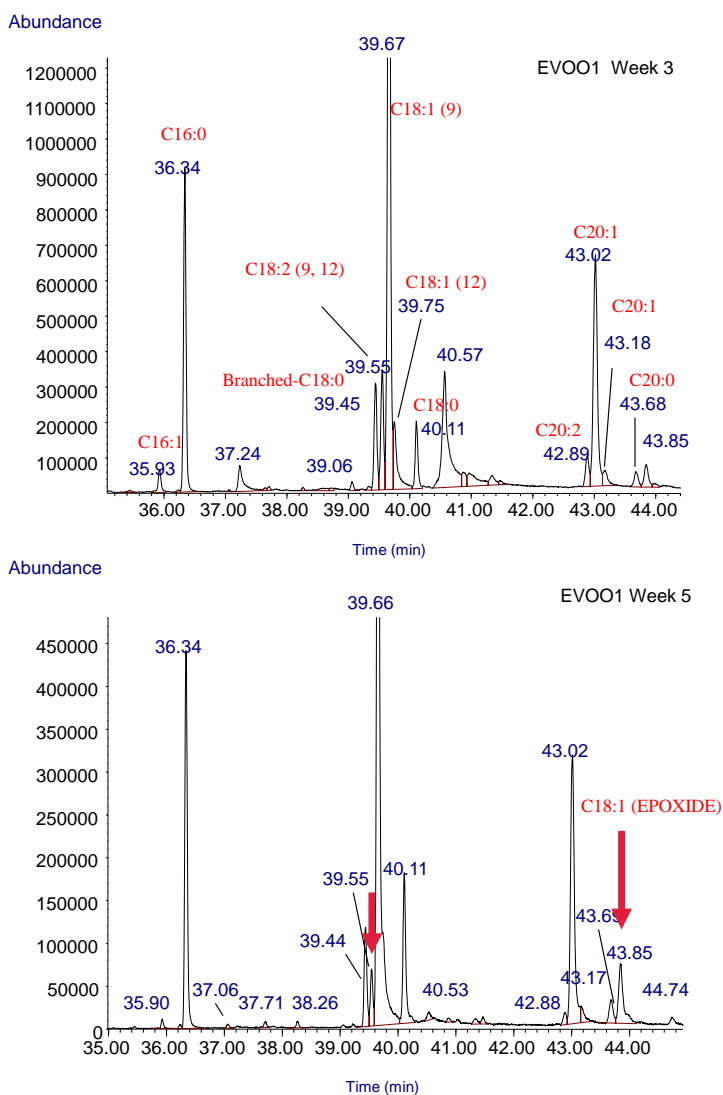


Figure 8. Gas Chromatography spectra showing the relative abundances of molecules in EVOO 1 on week 3 (top) and week 5 (bottom). All molecules are identified by Mass spectroscopy. Of significance is the reduction in C18:2(9,12) at 39.55 mins and increase in C18:1 at 43.85 mins on week 5. (CX:Y(a,b) represents X saturated bonds and Y unsaturated bonds on a carbon chain, where unsaturated bonds are at positions a and b.)

Table 7. Confusion matrix for data taken over 2 weeks using PCS 2-7

Prediction/Actual	1	2	3	4	5
1	29	1	0	0	0
2	1	29	0	0	0
3	0	0	30	0	0
4	0	0	0	30	0
5	0	0	0	0	30

#### 4. Conclusions

It is possible to use either solely Raman spectroscopy or solely fluorescence spectroscopy to discriminate and identify EVOO brands, that may assist to combat the counterfeiting and adulteration of EVOO. Combining Raman and fluorescence spectroscopic data gives a more complete analysis which could be employed in EVOO quality checks with respect to IOC standards. The use of a

compact portable Raman device obviates the need to use centralised laboratories for analysis and opens up the prospect for in field sensing. Importantly as our approach of Raman spectroscopy or fluorescence requires no sample labeling or particular preparation we believe these techniques are ideal for integration to in-line testing procedures in the future.

## 5. Acknowledgements

We thank the UK Engineering and Physical Sciences Research Council and the European Union FAMOS project (FP7 ICT, 317744) for funding. We acknowledge loan of the compact hand-held device from MSquared Lasers.

## References

- [1] Retrieved July 14, 2015 from <http://www.internationaloliveoil.org/estaticos/view/222-standards>
- [2] E.N. Frankel et al "Evaluation of Extra-Virgin Olive Oil Sold in California" UC Davis Olive Center **2011**
- [3] M. D. Kontogianni, D. B. Panagiotakos, C. Chrysohoou, C. Pitsavos, A. Zampelas, C. Stefanadis, *Clin. Cardiol.* **2007**; 30, 125–129
- [4] R. W. Owen, R. Haubner, G. Würtele, E. Hull, B Spiegelhalder, H. Bartsch, *Eur J Cancer Prev* **2004**; 13, 4, 319-26
- [5] K. W. Wahle, D Caruso, J. J. Ochoa, J.L Quiles, *Lipids* **2004**; 39, 12, 1223-31
- [6] W. Dong, Y. Zhang, B. Zhang, X. Wang, *Anal. Methods* **2012**; 4, 2772
- [7] G. Vlahov, P. Del Re, N. Simone, *J. Agric. Food. Chem* **2003**; 51, 19, 5612-5
- [8] J. C. Cancellia, S. C. Wang, P. Diaz-Rodriguez, G. Matute, J. D. Cancellia, D. Flynn, J. S. Torrecilla, *J. Agric. Food Chem* **2014**; 62, 10661–10665
- [9] E. Guzmán, V. Baeten, J. A. F. Pierna, J. A. García-Mesa, *Food Control* **2011**; 22, 2036-2940
- [10] Ayton.J., Mailer.R.J., Graham.K., "The Effect of Storage Conditions on Extra Virgin Olive Oil Quality," *RIRDC*; **2012** 12/024
- [11] R. M. El-Abassy, P. Donfack, A. Materny, *J. Am. Oil Chem. Soc* **2009**; 86, 6, 507-511
- [12] M.-Q. Zou, X.-F. Zhang, X.-H. Qi, H.-L. Ma, Y. Dong, C-W. Liu, X. Guo, H. Wang, *J. Agric. Food Chem* **2009**; 57, 14, 6001–6006
- [13] Retrieved March 14, 2015 from [www.oliveoilsource.com/page/chemical-characteristics](http://www.oliveoilsource.com/page/chemical-characteristics)
- [14] K. H. Levin, C. L. Tang, *Appl. Phys. Lett.* **1978**; 33, 817-819
- [15] A. P. Shreve, N. J. Cherepy, R. A. Mathies, *Appl. Spectrosc.* **1992**; 46, 4, 707-711
- [16] A. C. De Luca, M. Mazilu, A. Riches, C .S. Herrington, K. Dholakia, *Anal. Chem.* **2010**; 82, 738-745
- [17] M. Mazilu, A. C. De Luca, A. Riches, C. S. Herrington, K. Dholakia, *Opt. Express*, **2010**; 18, 11382-11395
- [18] M. Chen, N. McReynolds, E. C. Campbell, M. Mazilu, J. Barbosa, K. Dholakia, *PLoS ONE*, **(2015)**; 10, 5
- [19] J. De Gelder, K. De. Gussem, P. Vandenabeele, L. Moens, *J. Raman Spectrsc*, **2007**; 38, 9, 1133-1147